Traces of the deconfinend phase transition

Elena Bratkovskaya
(GSI, Darmstadt & ITP, Uni. Frankfurt)

In collaboration with Hamza Berrehrah, Wolfgang Cassing, Thorsten Steinert, Jörg Aichelin, Pol-Bernard Gossiaux, Pierre Moreau, Taesoo Song

"CPOD2017": Critical Point and Onset of Deconfinement"
Stony Brook University, Stony Brook, NY
August 7-11, 2017

The ‚holy grail‘ of heavy-ion physics:

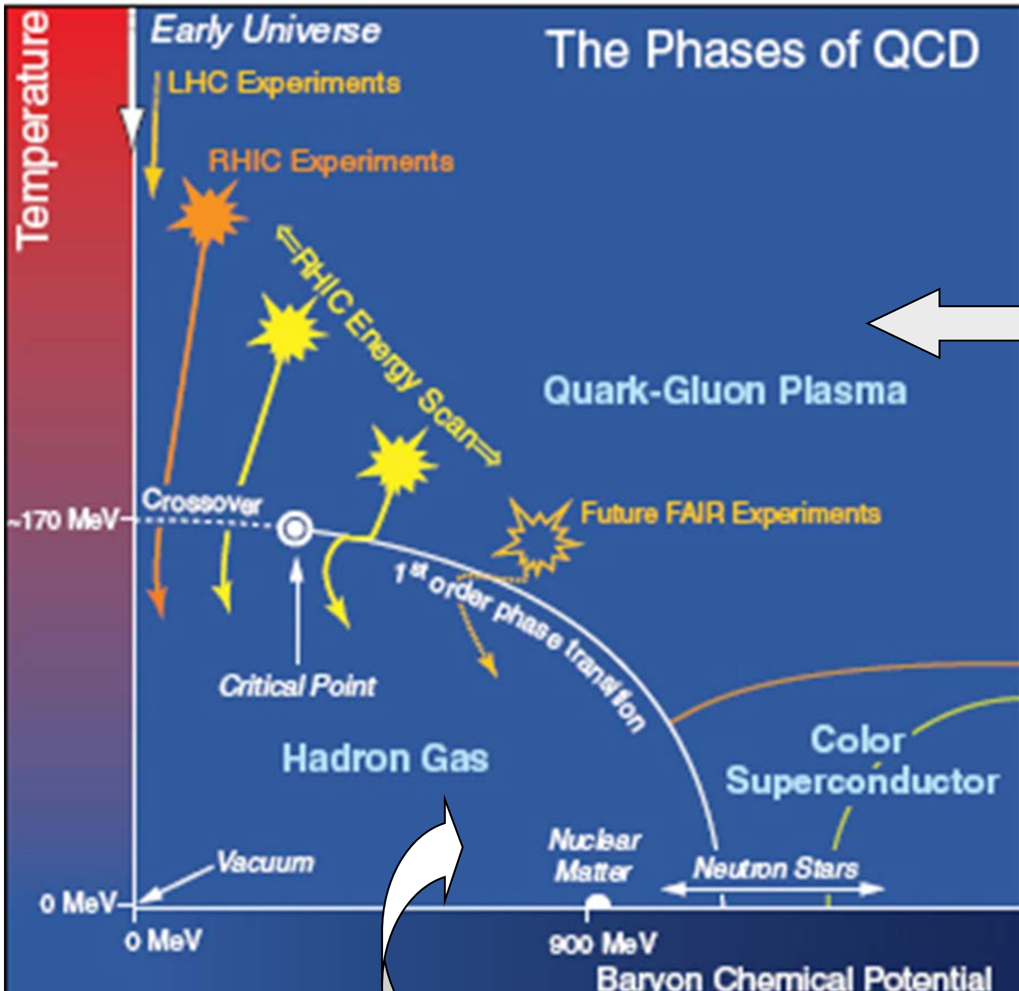

The phase diagram of QCD

- Study of the phase transition from hadronic to partonic matter – Quark-Gluon-Plasma

- Search for the critical point
- Search for signatures of chiral symmetry restoration
- Study of the in-medium properties of hadrons at high baryon density and temperature

Degrees-of-freedom of QGP

❖ lQCD gives QGP EoS at finate μ_B

! need to be interpreted in terms of degrees-of-freedom

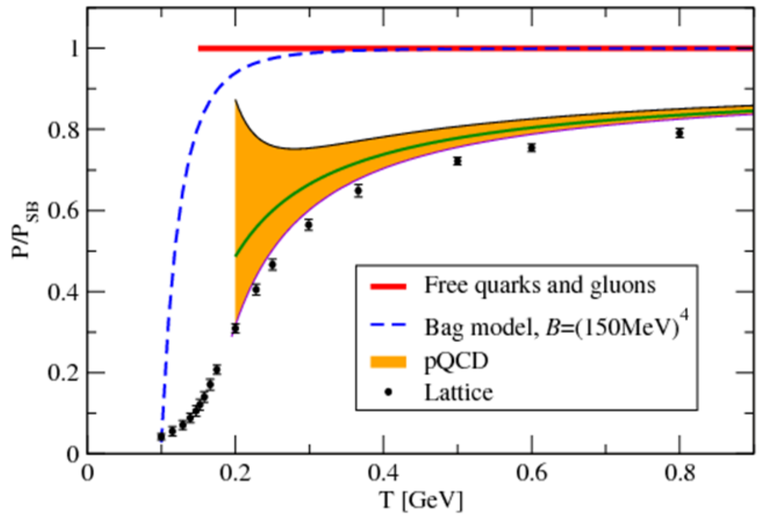

Non-perturbative QCD ← pQCD

pQCD:

- weakly interacting system
- massless quarks and gluons

Thermal QCD = QCD at high parton densities:

- strongly interacting system
- massive quarks and gluons

❖ Effective degrees-of-freedom

QGP thermodynamics: from lQCD to QP/DQP

❖ **Effective degrees-of-freedom ➔ quasi-particles**

➢ **Grand canonical potential Ω in propagator (D,S) representation (2PI):**

$$\beta\Omega[D,S] = \underbrace{\frac{1}{2}\mathrm{Tr}[\ln D^{-1} - \Pi D]}_{\text{bosons}} - \underbrace{\mathrm{Tr}[\ln S^{-1} + \Sigma S]}_{\text{fermions}} + \Phi[D,S]$$

Self-energies:

$$\frac{\delta\Phi}{\delta D} = \frac{1}{2}\Pi$$

$$\frac{\delta\Phi}{\delta S} = -\Sigma$$

Cf. J.P. Blaizot et al, PRD 63 (2001) 065003

1. Weakly interacting on-shell Quasi-Particles (QP):

QP: $p_{\mathrm{QP}}(T) = p^{\mathrm{id\,gas}}(T, m^2(T)) + B(m^2(T))$ $\qquad \frac{\partial p_{\mathrm{QP}}(T,m^2)}{\partial m^2} = 0$

➢ **Different QP versions:**

- Effective thermal masses *(Peshier et al., Greco et al, Bluhm et al,…)*
- Polyakov loop models (*Pisarski*)
- . . .

Bag constant: $B(m^2(T))$ calculated self-consistently to render QGP thermodynamics consistently

Gorenstein & Yang, PRD **52,** 5206 **(**1995)

➢ **Effective** coupling, IR enhancement, massive transverse gluons

$$\alpha(T) = \frac{4\pi/11}{\ln\left(\lambda\frac{T+T_s}{T_c}\right)^2} \qquad m^2(T) = \frac{1}{2}\,4\pi\alpha(T)T^2$$

QGP thermodynamics: from lQCD to QP/DQP

❖ Effective degrees-of-freedom ➔ quasi-particles

Peshier, Cassing, PRL 94 (2005) 172301

2. Strongly interacting Quasi-Particles (DQP):

- **QPM ➔ DQPM**

- **small entropy near T_c: large quasiparticle mass, large coupling from lQCD ➔ large quasiparticle width γ**

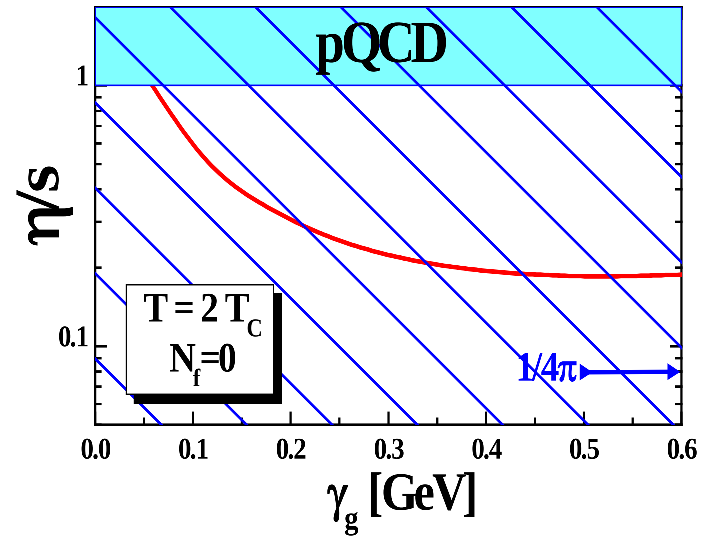

- **Grand canonical potential Ω in propagator representation (2PI) ➔ thermal properties of the system:**

$$\Omega/V = -P \qquad d\Omega = -SdT - PdV - Nd\mu \qquad S = -\frac{\partial\Omega}{\partial T} \qquad N = -\frac{\partial\Omega}{\partial\mu} \qquad P = -\frac{\partial\Omega}{\partial V}$$

1. Determine entropy *S*, pressure *P* for DQP

2. Fit *S*, *P* from DQP with *S*, *P* from lQCD

➔ Properties of quasi-particles

Dynamical QuasiParticle Model (DQPM) - Basic ideas:

DQPM describes QCD properties in terms of ‚resumed' single-particle Green's functions (propagators) – in the sense of a two-particle irreducible (2PI) approach:

gluon propagator: $\Delta^{-1} = P^2 - \Pi$ & quark propagator $S_q^{-1} = P^2 - \Sigma_q$

gluon self-energy: $\Pi = M_g^2 - i2\gamma_g\omega$ & quark self-energy: $\Sigma_q = M_q^2 - i2\gamma_q\omega$

(scalar approximation)

- the resumed properties are specified by complex (retarded) self-energies:
- the real part of self-energies (Σ_q, Π) describes a dynamically generated mass (M_q,M_g);
- the imaginary part describes the interaction width of partons (γ_q, γ_g)
- Spectral functions : $A_q \sim Im S_q^{ret}, \quad A_g \sim Im \Delta^{ret}$

- Entropy density of interacting bosons and fermions in the quasiparticle limit (2PI) (G. Baym 1998):

QGP

$$s^{dqp} = -d_g \int \frac{d\omega}{2\pi} \frac{d^3p}{(2\pi)^3} \frac{\partial n_B}{\partial T} \left(\mathrm{Im} \ln(-\Delta^{-1}) + \mathrm{Im}\, \Pi\, \mathrm{Re}\, \Delta \right) \quad \text{gluons}$$

$$- d_q \int \frac{d\omega}{2\pi} \frac{d^3p}{(2\pi)^3} \frac{\partial n_F((\omega - \mu_q)/T)}{\partial T} \left(\mathrm{Im} \ln(-S_q^{-1}) + \mathrm{Im}\, \Sigma_q\, \mathrm{Re}\, S_q \right) \quad \text{quarks}$$

$$- d_{\bar{q}} \int \frac{d\omega}{2\pi} \frac{d^3p}{(2\pi)^3} \frac{\partial n_F((\omega + \mu_q)/T)}{\partial T} \left(\mathrm{Im} \ln(-S_{\bar{q}}^{-1}) + \mathrm{Im}\, \Sigma_{\bar{q}}\, \mathrm{Re}\, S_{\bar{q}} \right) \quad \text{antiquarks}$$

A. Peshier, W. Cassing, PRL 94 (2005) 172301; Cassing, NPA 791 (2007) 365: NPA 793 (2007)

DQPM (T)

DQPM(T): properties of quasiparticles

Properties of interacting quasi-particles: massive quarks and gluons (g, q, q_{bar}) with Lorentzian spectral functions :

$$A(\omega,\mathbf{p}) = \frac{\gamma}{E}\left(\frac{1}{(\omega-E)^2+\gamma^2} - \frac{1}{(\omega+E)^2+\gamma^2}\right)$$

$$E^2 = p^2 + M^2 - \gamma^2$$

- Modeling of the quark/gluon masses and widths → HTL limit at high T

masses: $$m_g^2 = \frac{g^2}{6}\left(N_c + \frac{1}{2}N_f\right)T^2\,, \qquad m_q^2 = g^2\frac{N_c^2-1}{8N_c}T^2$$

widths: $$\gamma_g = \frac{1}{3}N_c\frac{g^2 T}{8\pi}\ln\left(\frac{2c}{g^2}+1\right)\,, \quad \gamma_q = \frac{1}{3}\frac{N_c^2-1}{2N_c}\frac{g^2 T}{8\pi}\ln\left(\frac{2c}{g^2}+1\right)$$

- running coupling (pure glue):

$$\alpha_s(T) = \frac{g^2(T)}{4\pi} = \frac{12\pi}{(11N_c - 2N_f)\ln[\lambda^2(T/T_c - T_s/T_c)^2]}$$

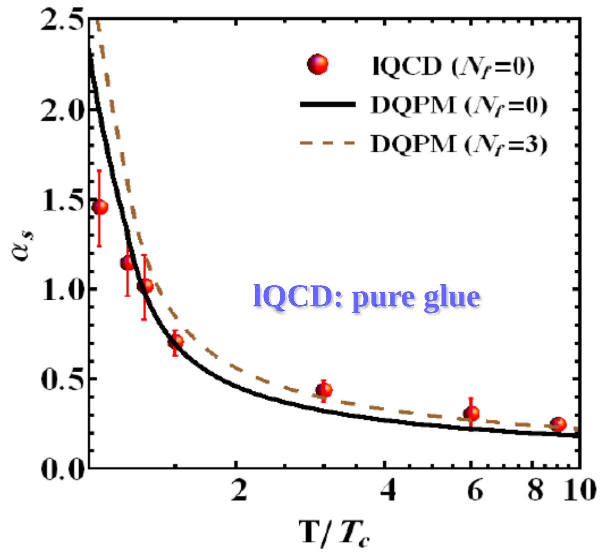

- fit to lattice (lQCD) results (e.g. entropy density)

with 3 parameters: T_s/T_c=0.46; c=28.8; λ=2.42 (for pure glue N_f=0)

Peshier, Cassing, PRL 94 (2005) 172301;
Cassing, NPA 791 (2007) 365: NPA 793 (2007)

DQPM at finite T and μ_q=0

➢ fit to lattice (lQCD) results

* BMW lQCD data S. Borsanyi et al., JHEP 1009 (2010) 073

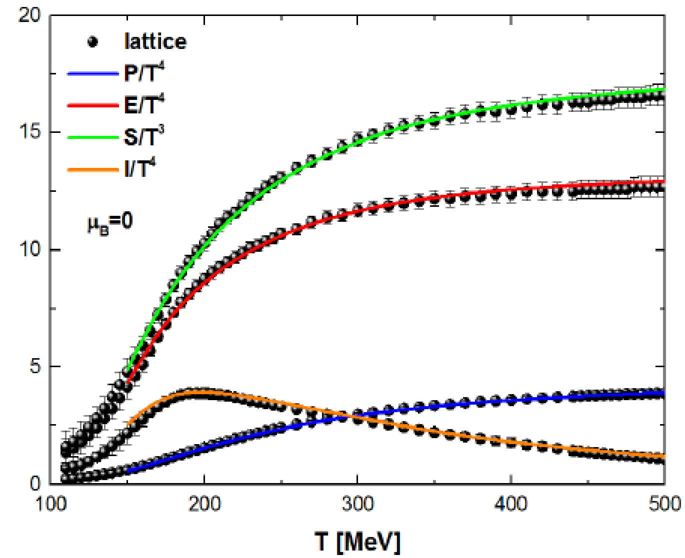

➔ Quasiparticle properties:

- large width and mass for gluons and quarks

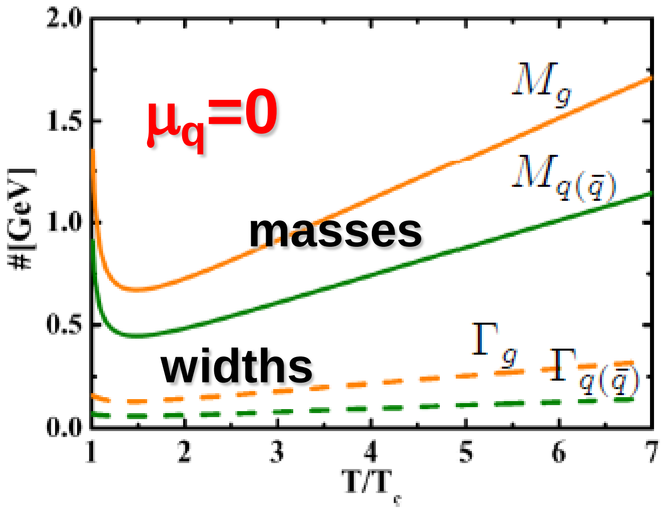

T_C=158 MeV
ε_C=0.5 GeV/fm^3

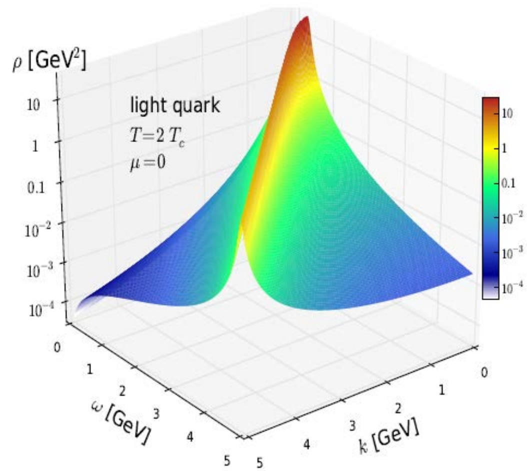

DQPM

- matches well lattice QCD
- provides mean-fields (1PI) for gluons and quarks as well as effective 2-body interactions (2PI)
- gives transition rates for the formation of hadrons

➔ microscopic dynamical transport approach PHSD

Peshier, Cassing, PRL 94 (2005) 172301; Cassing, NPA 791 (2007) 365: NPA 793 (2007)

Traces of the QGP in observables in high energy heavy-ion collisions

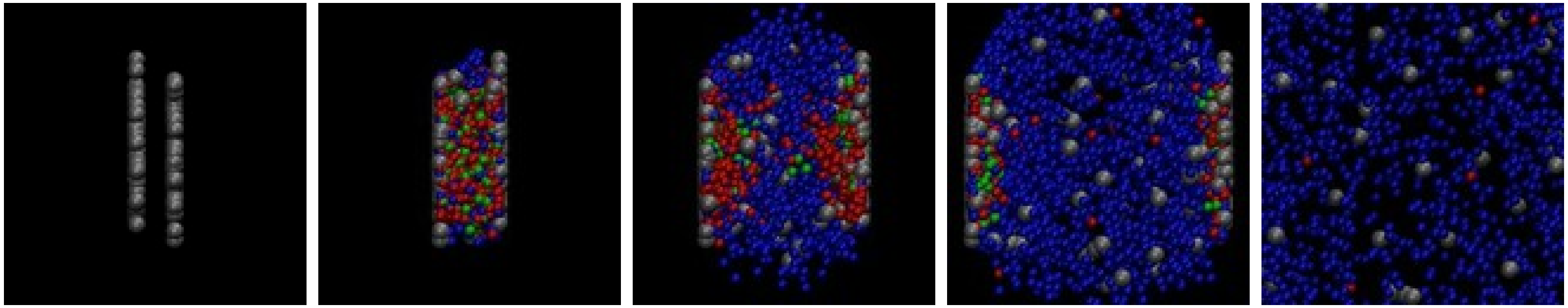

https://fias.uni-frankfurt.de/~phsd-project/PHSD/index1.html

Basic idea: off-shell PHSD approach

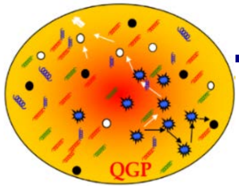

QGP in equilibrium

Dynamical QuasiParticle Model (DQPM):

fitted to → **lQCD**

controled by lQCD!

Quasiparticle properties:
‚resummed' self-energies, propagators
➔ Calculation of cross sections

⇒ **Calculation of transport coefficients in equilibrium** $\eta, \zeta, \sigma_0, ..$

DQPM: consider the effects of the nonperturbative nature of the strongly interacting quark-gluon plasma (sQGP) constituents (vs. pQCD models)

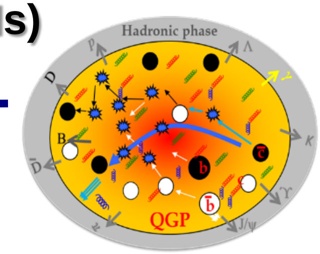

QGP out-of equilibrium ⇔ HIC

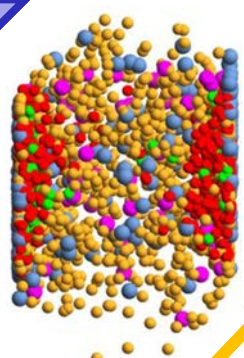

Parton-Hadron-String-Dynamics (PHSD)

controled by → **experimental data + lQCD**

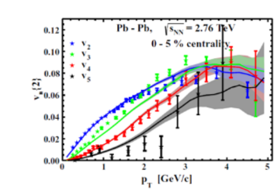

- **Partonic interactions → DQPM**
- **hadronic interactions → hadron physics**
- *** In-medium hadronic interactions → many-body physics: G-matrix**

Partonic energy fraction in central A+A

Time evolution of the partonic energy fraction vs energy

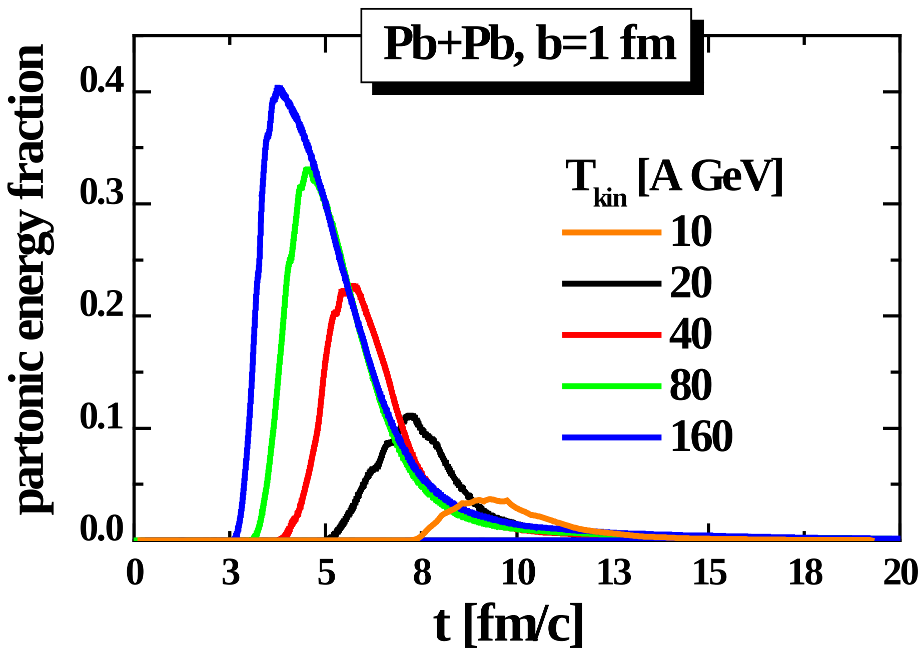

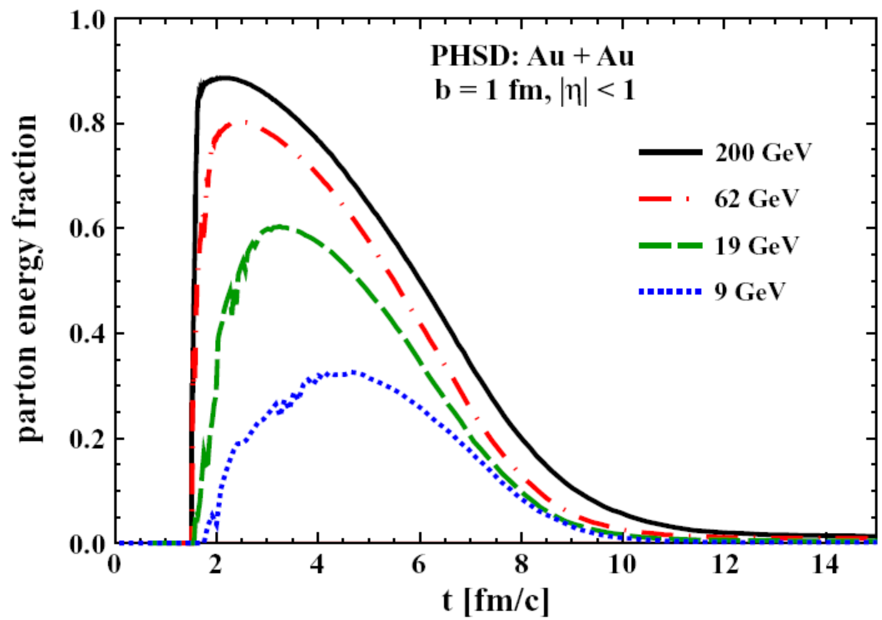

- Strong increase of partonic phase with energy from AGS to RHIC

- SPS: Pb+Pb, 160 A GeV: only about 40% of the converted energy goes to partons; the rest is contained in the large hadronic corona and leading partons
- RHIC: Au+Au, 21.3 A TeV: up to 90% - QGP

W. Cassing & E. Bratkovskaya, NPA 831 (2009) 215
V. Konchakovski et al., Phys. Rev. C 85 (2012) 011902

Transverse mass spectra from SPS to RHIC

Central Pb + Pb at SPS energies

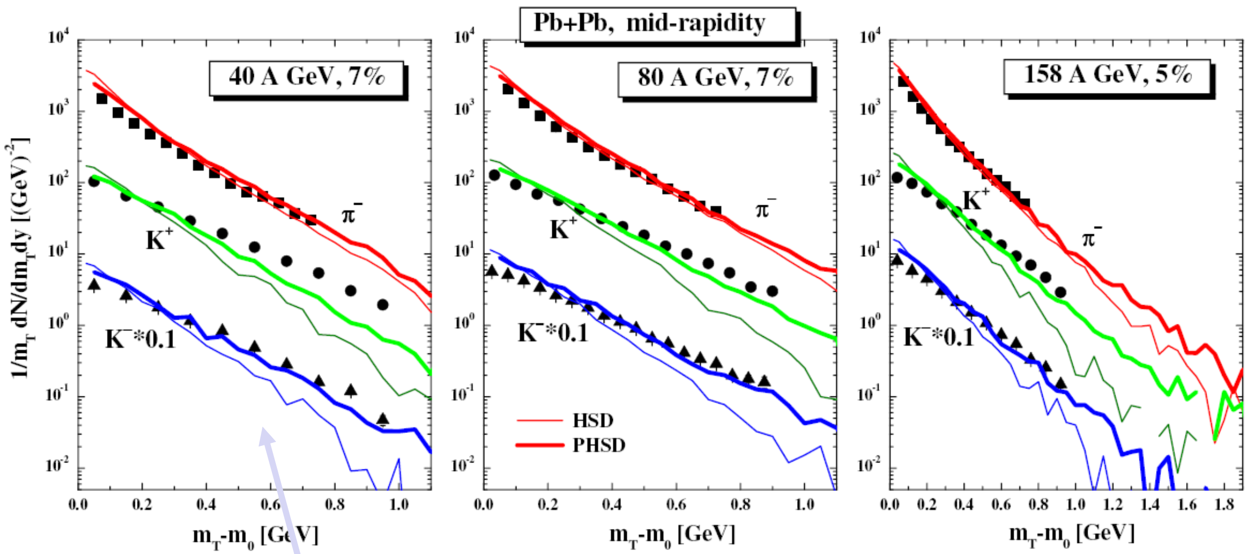

Central Au+Au at RHIC

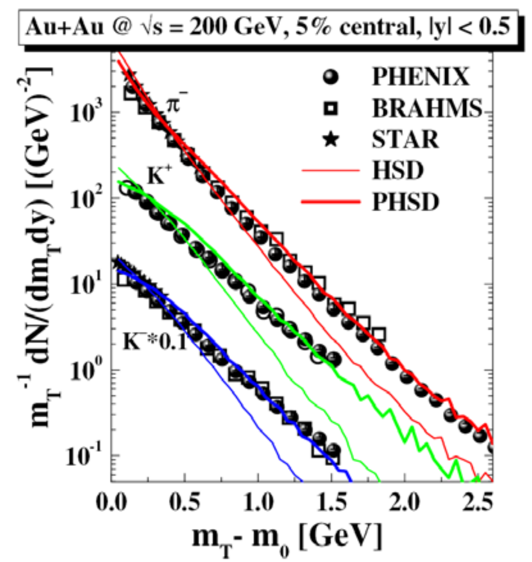

- ❑ PHSD gives harder m_T spectra and works better than HSD (wo QGP) at high energies – RHIC, SPS (and top FAIR, NICA)
- ❑ however, at low SPS (and low FAIR, NICA) energies the effect of the partonic phase decreases due to the decrease of the partonic fraction

W. Cassing & E. Bratkovskaya, NPA 831 (2009) 215
E. Bratkovskaya, W. Cassing, V. Konchakovski, O. Linnyk, NPA856 (2011) 162

Elliptic flow v_2 vs. collision energy for Au+Au

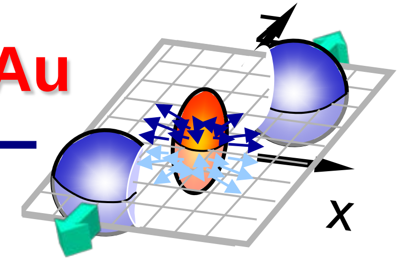

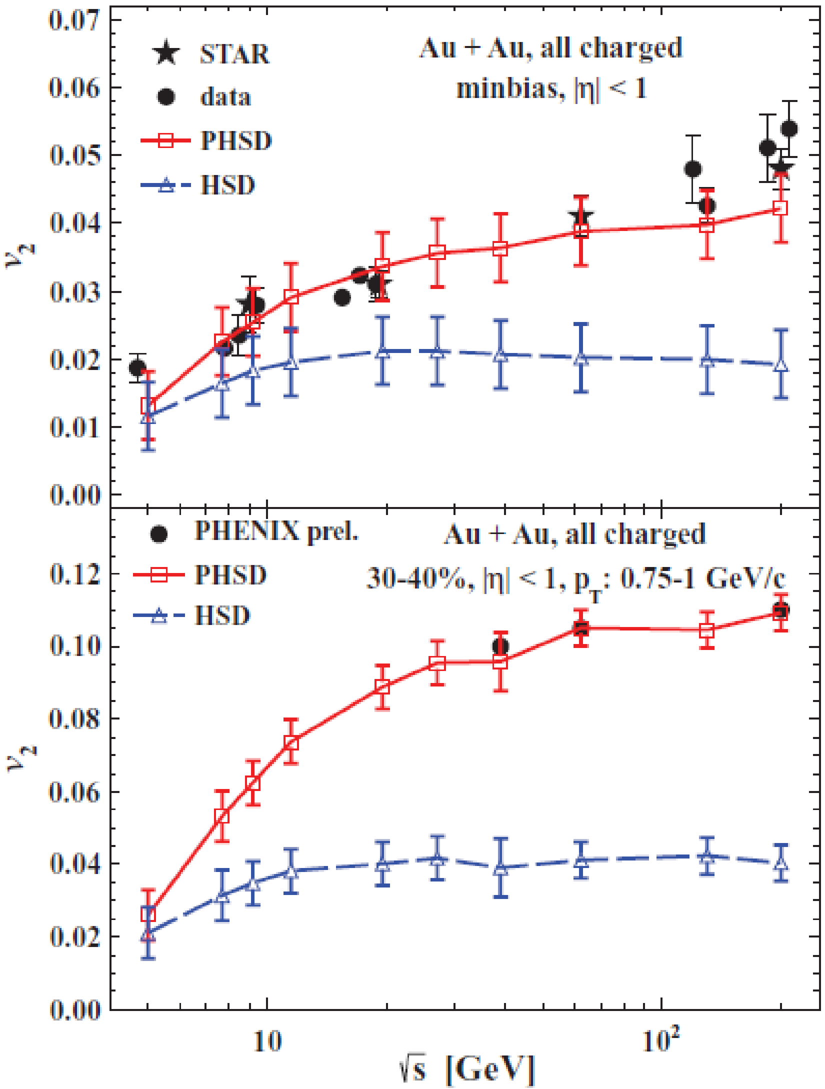

$$\frac{dN}{d\varphi} \propto \left(1 + 2\sum_{n=1}^{+\infty} v_n \cos\left[n(\varphi - \psi_n)\right]\right)$$

$$v_n = \left\langle \cos n\left(\varphi - \psi_n\right)\right\rangle, \quad n = 1,2,3..,$$

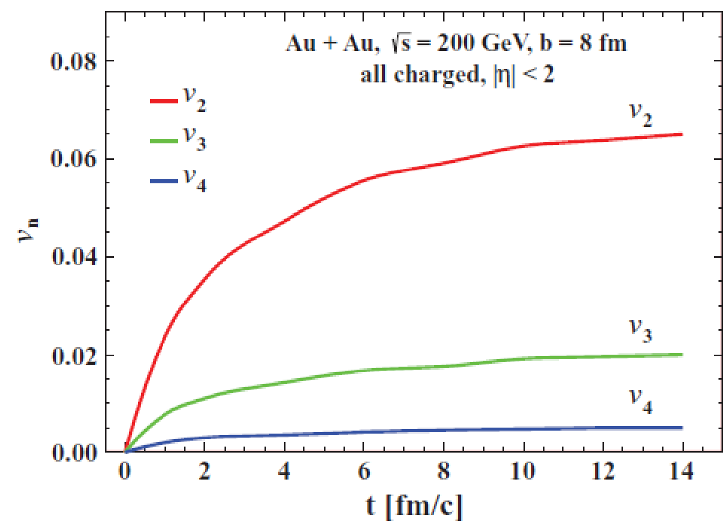

- v_2 in PHSD is larger than in HSD due to the repulsive scalar mean-field potential $U_s(\rho)$ for partons
- v_2 grows with bombarding energy due to the increase of the parton fraction

V. Konchakovski, E. Bratkovskaya, W. Cassing, V. Toneev, V. Voronyuk, Phys. Rev. C 85 (2012) 011902

Extended DQPM (T, μ_q)

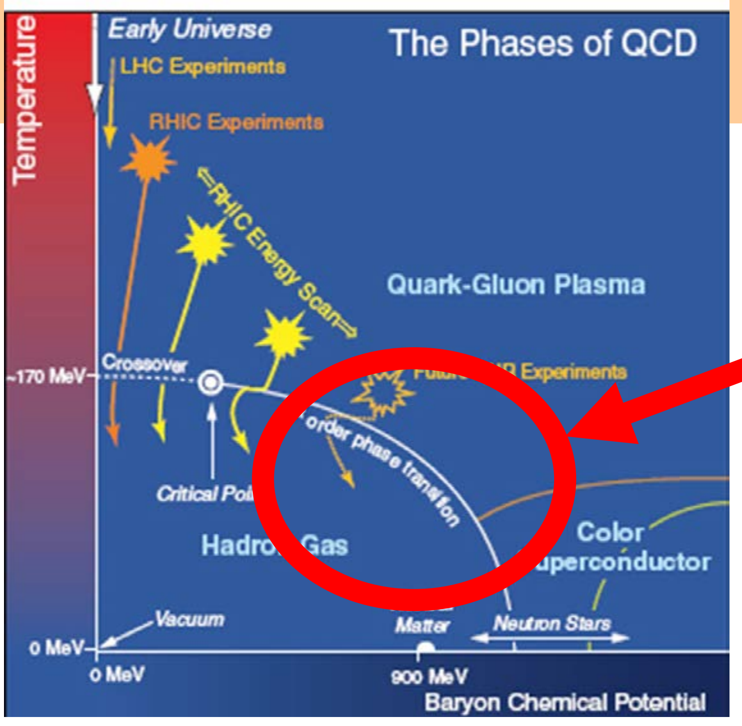

finite μ_q

DQPM at finite (T, μ_q): scaling hypothesis

Talk by Jana G□unther

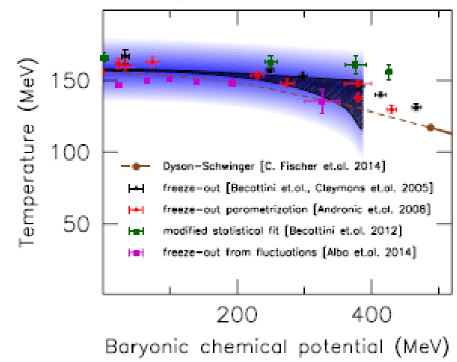

- **Scaling hypothesis for the effective temperature T***
  for $N_f = N_c = 3$

$$\mu_u = \mu_d = \mu_s = \mu_q$$

$$T^{*2} = T^2 + \frac{\mu_q^2}{\pi^2}$$

- **Coupling constant:**

$$g(T/T_c(\mu=0)) \longrightarrow g(T^*/T_c(\mu))$$

- **Critical temperature $T_c(\mu_q)$:**

obtained by requiring a constant energy density ε for the system at $T=T_c(\mu_q)$ where ε at $T_c(\mu_q=0)$=158 GeV is fixed by lQCD at μ_q=0

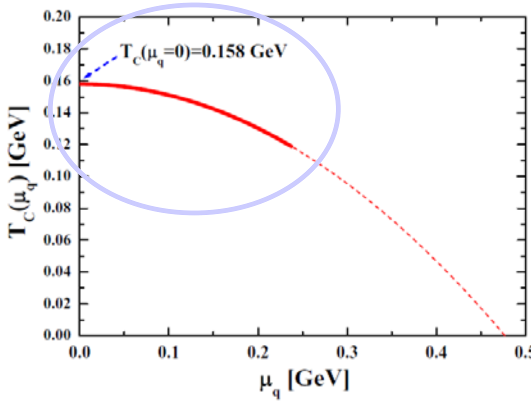

$$\frac{T_c(\mu_q)}{T_c(\mu_q=0)} = \sqrt{1-\alpha\,\mu_q^2} \approx 1-\alpha/2\,\mu_q^2+\cdots$$

$$\alpha \approx 8.79\ \mathrm{GeV}^{-2}$$

! Consistent with lattice QCD:

lQCD: C. Bonati et al., PRC90 (2014) 114025

$$\frac{T_c(\mu_B)}{T_c} = 1-\kappa\left(\frac{\mu_B}{T_c}\right)^2+\cdots$$

lQCD $\kappa = 0.013(2)$ ⟷ $\kappa_{DQPM} \approx 0.0122$

H. Berrehrah et al, PRC 93 (2016) 044914, Int.J.Mod.Phys. E25 (2016) 1642003,

DQPM at finite (T, μ_q): quasiparticle masses and widths

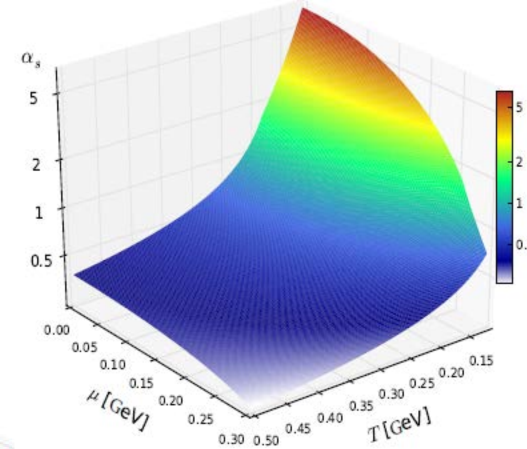

Coupling constant:

$$g^2(T^\star/T_c(\mu_q)) = \frac{48\pi^2}{(11N_c - 2N_f)\ln\left(\lambda^2(\frac{T^\star}{T_c(\mu_q)} - \frac{T_s}{T_c(\mu_q)})^2\right)}$$

Quark and gluon masses:

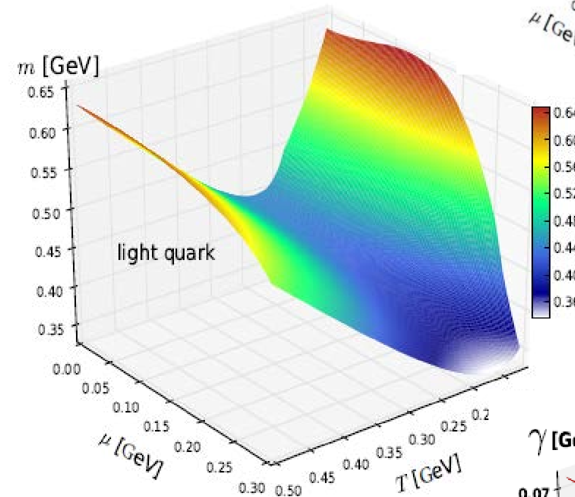

$$M_g^2(T^\star,\mu_q) = \frac{g^2(T^\star/T_c(\mu_q))}{6}(N_c + \frac{1}{2}N_f)\, T^{\star 2},$$

$$M_q^2(T^\star,\mu_q) = \frac{N_c^2-1}{8N_c} g^2(T^\star/T_c(\mu_q))\, T^{\star 2},$$

Quark and gluon widths:

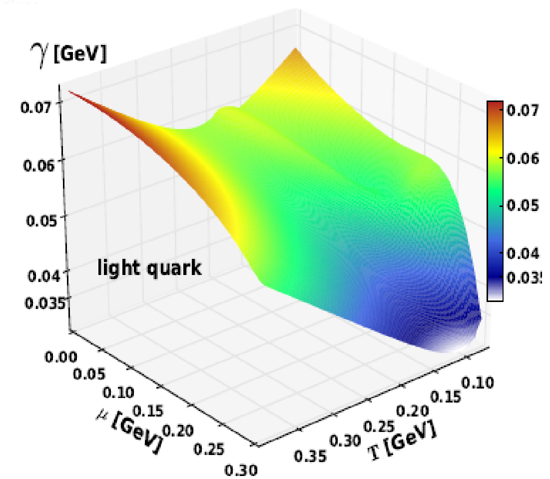

$$\gamma_g(T,\mu_q) = \frac{1}{3}N_c \frac{g^2(T^*/T_c(\mu_q))}{8\pi} T \ \ln\left(\frac{2c}{g^2(T^*/T_c(\mu_q))} + 1\right),$$

$$\gamma_q(T,\mu_q) = \frac{1}{3}\frac{N_c^2-1}{2N_c}\frac{g^2(T^*/T_c(\mu_q))}{8\pi} T \ \ln\left(\frac{2c}{g^2(T^*/T_c(\mu_q))} + 1\right).$$

DQPM: thermodynamics at finite (T, μ_q)

❑ Entropy density at finite T

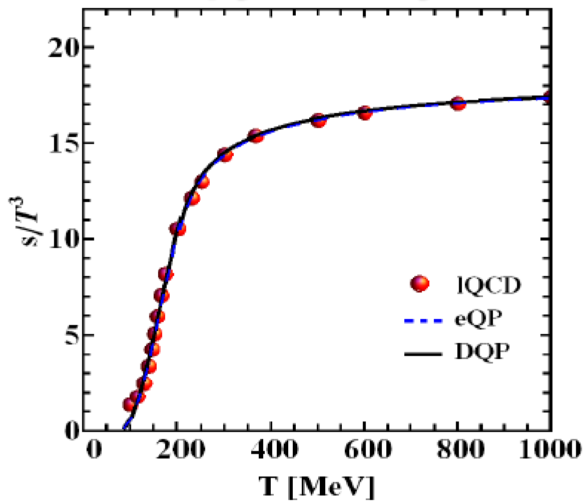

Entropy density at finite (T, μ_q)

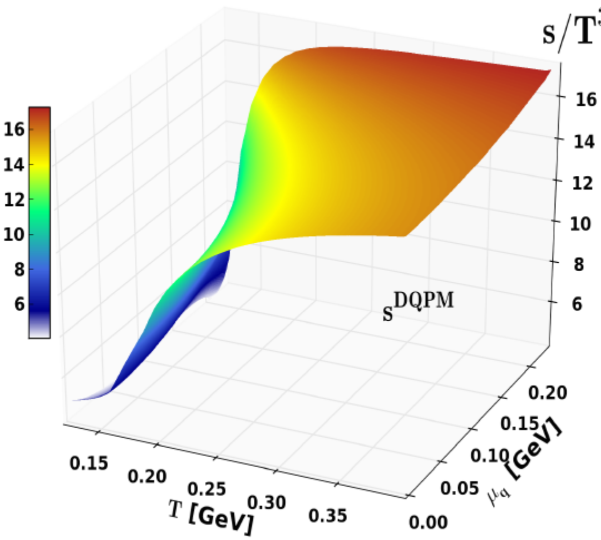

❑ Energy density at finite T

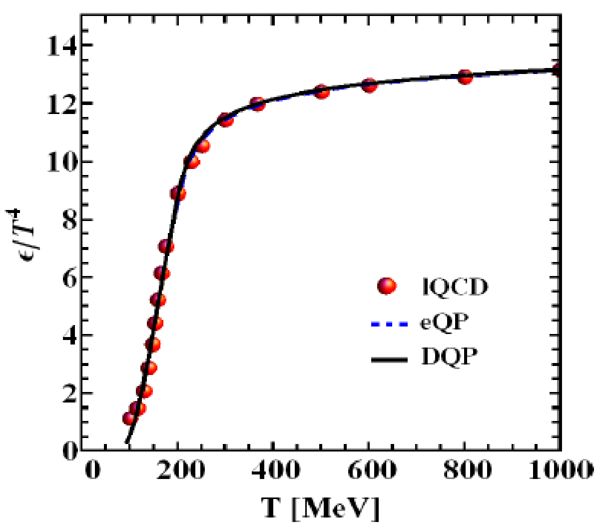

Energy density at finite (T, μ_q)

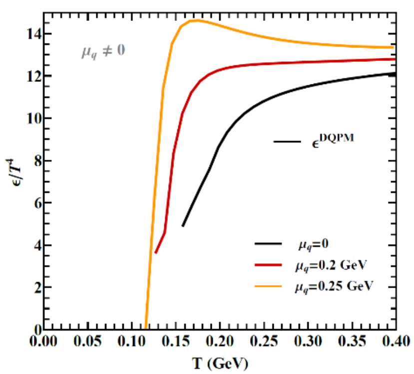

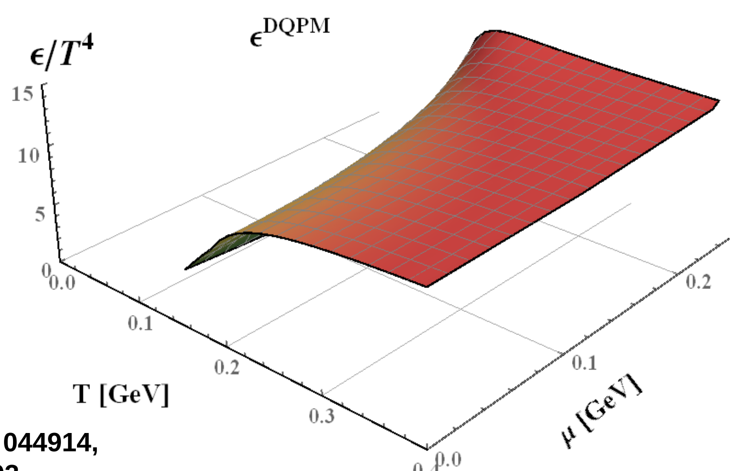

H. Berrehrah et al, PRC 93 (2016) 044914,
Int.J.Mod.Phys. E25 (2016) 1642003,

DQPM(T, μ_q): n_B , χ_q

- **Baryon number density n_B , susceptibilities χ_q at finite (T, μ)**

$$\chi_q(T) = \frac{\partial n_q}{\partial \mu_q}\bigg|_{\mu_q=0}; \qquad \chi_q(T,\mu_q) = \frac{1}{9}\frac{\partial n_B}{\partial \mu_B}. \qquad \chi_2(T) = \frac{1}{9}\frac{1}{T^2}\frac{\partial n_q(T,\mu_q)}{\partial \mu_q}\bigg|_{\mu_q=0} = \frac{1}{9}\frac{\chi_q(T)}{T^2}$$

for 3 flavours with $\mu_u = \mu_d = \mu_s = \mu_q$

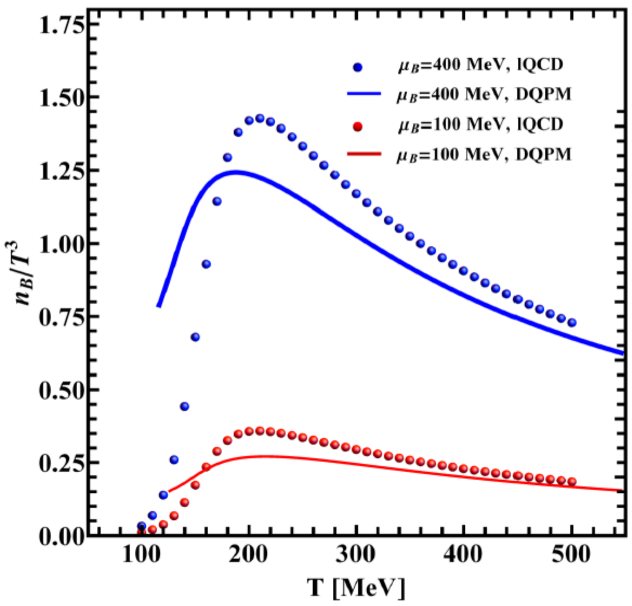

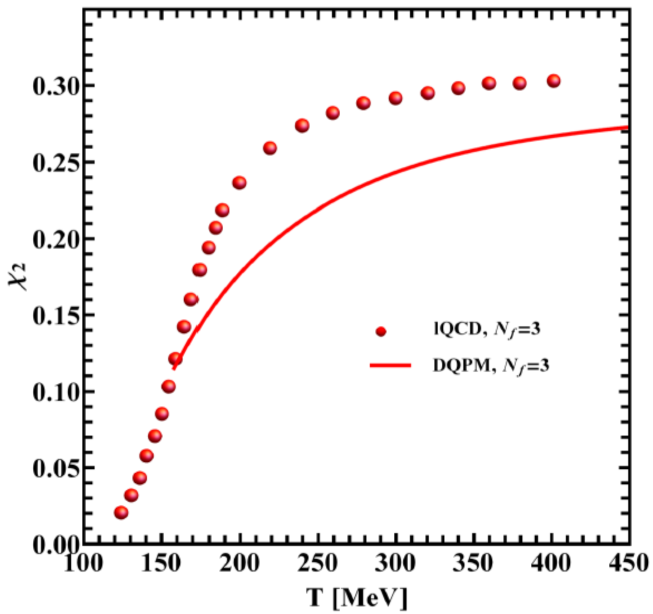

- **Comparison to lQCD : n_B, χ_q from DQPM is lower then lQCD data**
- **Quarks / gluons from DQPM are too heavy?**

H. Berrehrah et al, PRC 93 (2016) 044914, Int.J.Mod.Phys. E25 (2016) 1642003,

DQPM* (T, μ_q, p)

DQPM* at finite (T, μ_q, p): quasiparticle masses and widths

- **Momentum dependent Lorentzian spectral function :**

H. Berrehrah et al, PRC 93 (2016) 044914, arXiv:1512.06909; Int.J.Mod.Phys. E25 (2016) 1642003, arXiv:1605.02371

$$\rho_i(\omega,\boldsymbol{p}) = \frac{\gamma_i(\boldsymbol{p})}{\tilde{E}_i(\boldsymbol{p})}\left(\frac{1}{(\omega-\tilde{E}_i(\boldsymbol{p}))^2+\gamma_i^2(\boldsymbol{p})} - \frac{1}{(\omega+\tilde{E}_i(\boldsymbol{p}))^2+\gamma_i^2(\boldsymbol{p})}\right)$$

$$\tilde{E}_i^2(\boldsymbol{p}) = \boldsymbol{p}^2 + M_i^2(\boldsymbol{p}) - \gamma_i^2(\boldsymbol{p}) \text{ for } i \in [g,q,\bar{q}].$$

- ***p* dependence of $m_{q,\,g}$ inspired from Dyson-Schwinger results**

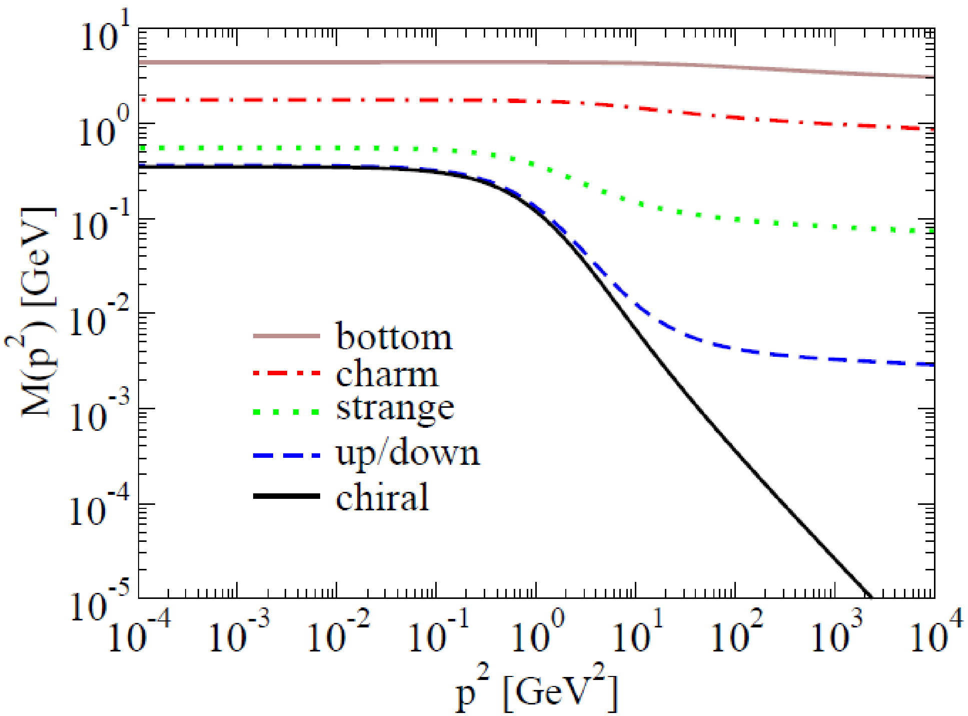

Ch.S. Fischer J. Phys. G: Nucl. Part. Phys. 32 (2006) R253–R291

DQPM* at finite (T, μ_q, p): quasiparticle masses and widths

H. Berrehrah et al, PRC 93 (2016) 044914, arXiv:1512.06909; Int.J.Mod.Phys. E25 (2016) 1642003, arXiv:1605.02371

❑ Quark and gluon masses:

$$M_g(T,\mu_q,p) = \left(\frac{3}{2}\right)\left[\frac{g^2(T^\star/T_c(\mu_q))}{6}\left[(N_c+\frac{N_f}{2})T^2+\frac{N_c}{2}\sum_q\frac{\mu_q^2}{\pi^2}\right]\right]^{1/2}\times h(\Lambda_g,p)+m_{\chi g}\ ,$$

$$M_{q,\bar{q}}(T,\mu_q,p) = \left[\frac{N_c^2-1}{8N_c}\,g^2(T^\star/T_c(\mu_q))\left[T^2+\frac{\mu_q^2}{\pi^2}\right]\right]^{1/2}\times h(\Lambda_q,p)+m_{\chi q}\ ,$$

$$h(\Lambda,p) = \left[\frac{1}{1+\Lambda(T_c(\mu_q)/T^\star)p^2}\right]^{1/2}$$

❑ Quark and gluon widths:

$$\Lambda_g(T_c(\mu_q)/T^\star) = 5\ \ (T_c(\mu_q)/T^\star)^2\ \mathrm{GeV}^{-2}$$

$$\Lambda_q(T_c(\mu_q)/T^\star) = 12\ \ (T_c(\mu_q)/T^\star)^2\ \mathrm{GeV}^{-2}$$

$$\gamma_g(T,\mu_q,p) = N_c\,\frac{g^2(T^\star/T_c(\mu_q))}{8\pi}\,T\,\ln\left(\frac{2c}{g^2(T^\star/T_c(\mu_q))}+1.1\right)^{3/4}\times h(\Lambda_g,p)\ ,$$

$$\gamma_{q,\bar{q}}(T,\mu_q,p) = \frac{N_c^2-1}{2N_c}\,\frac{g^2(T^\star/T_c(\mu_q))}{8\pi}\,T\ln\left(\frac{2c}{g^2(T^\star/T_c(\mu_q))}+1.1\right)^{3/4}\times h(\Lambda_q,p)$$

The final quark masses for the limits $p\to 0$ and $T=0$ or for $p\to\infty$

$m_{\chi q} = 0.003$ GeV for u, d quarks and $m_{\chi q} = 0.06$ GeV for s quarks

The gluon condensate: $m_{\chi g} = 0.5$ GeV

❑ Effective temperature T* for $N_f = N_c = 3$ (as in extended DQPM)

$$T^{*2} = T^2 + \frac{\mu_q^2}{\pi^2}$$

DQPM* at finite (T, μ_q,p): quasiparticle masses and widths

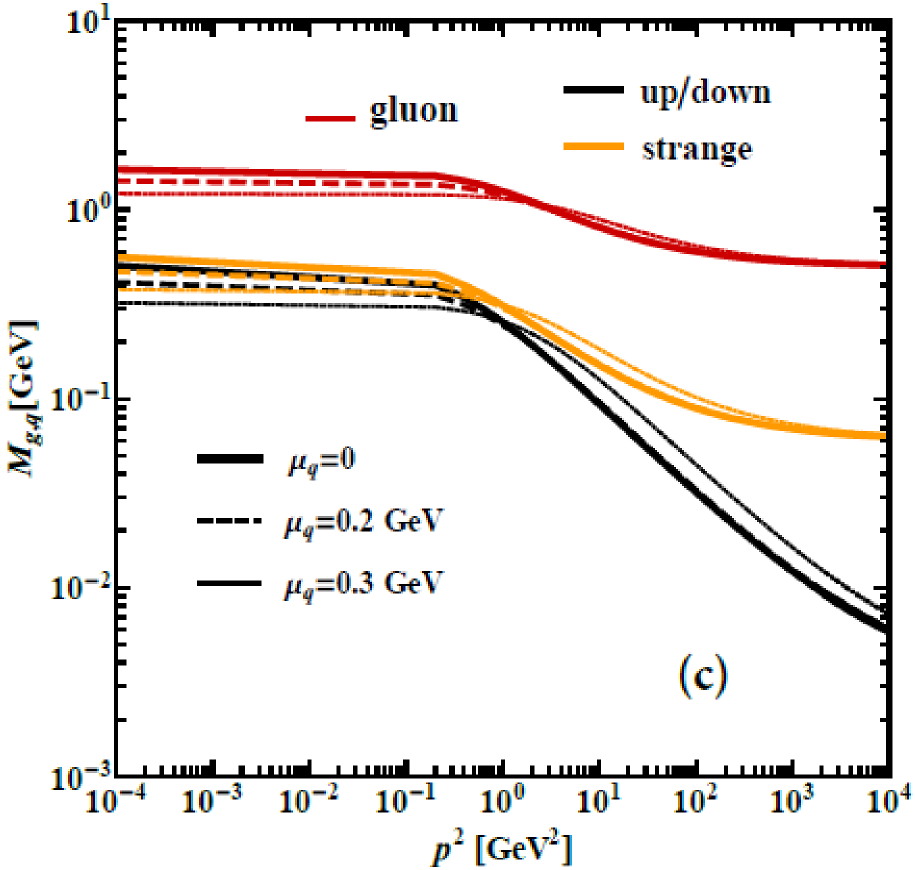

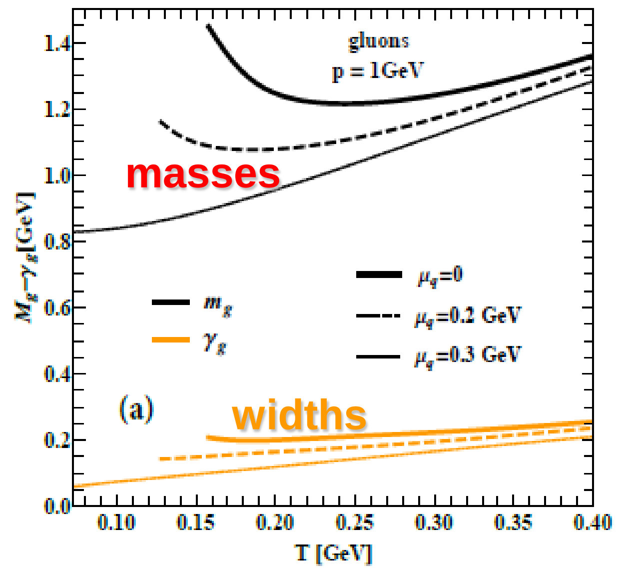

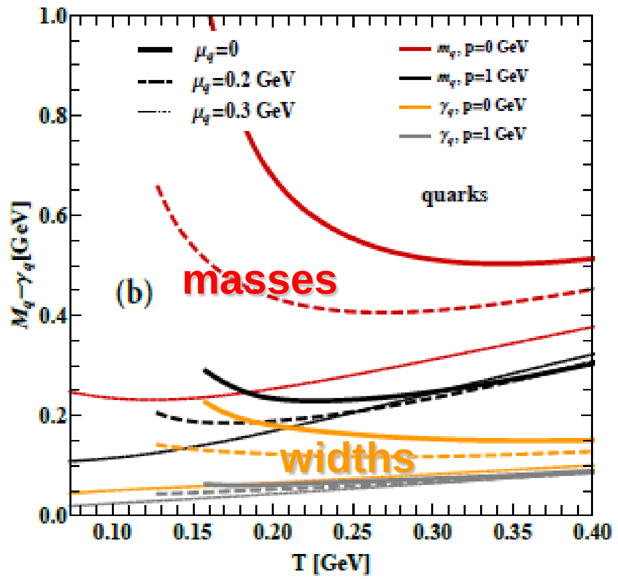

- **With increasing *p* momenta: $M_{q,g}$ and $\gamma_{q,g}$ decrease at T, μ_q**
- **$\mu_q = 0$ → finite μ_q: decrease of $M_{q,g}$ and $\gamma_{q,g}$**

H. Berrehrah et al, PRC 93 (2016) 044914, arXiv:1512.06909;
Int.J.Mod.Phys. E25 (2016) 1642003, arXiv:1605.02371

QGP Thermodynamics from DQPM* (T, μ_q,p)

❑ EoS from DQPM* at finite (T, μ_B)

Nf=3; lQCD, Sz. Borsanyi et al., JHEP08(2012)053

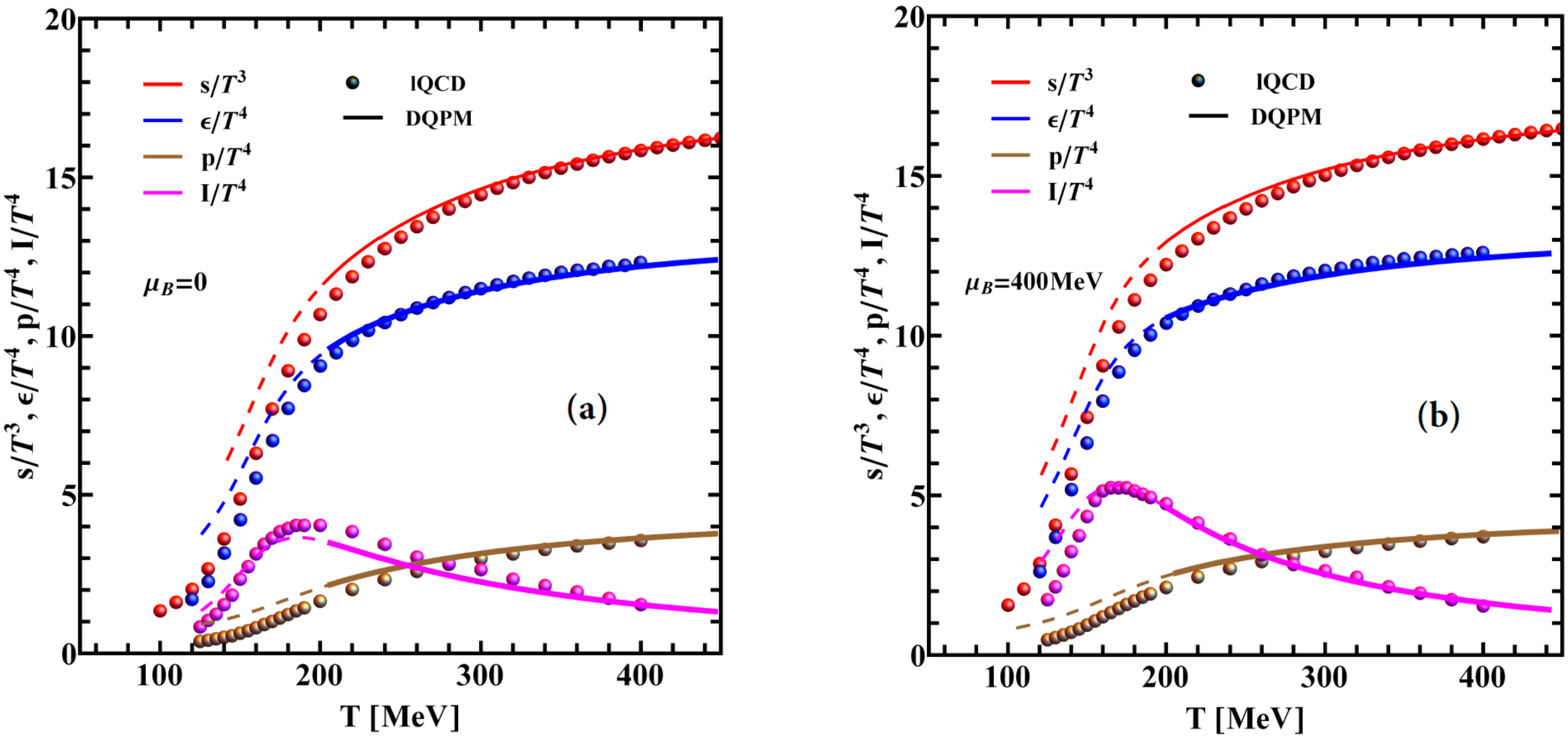

- High T (T>1.2 $T_c(\mu)$): very good agreement with the lattice data
- Low T (T<1.2 $T_c(\mu)$): some deviations → additional hadronic d.o.f in the crossover region ?

H. Berrehrah et al, PRC 93 (2016) 044914, arXiv:1512.06909; Int.J.Mod.Phys. E25 (2016) 1642003, arXiv:1605.02371

QGP Thermodynamics from DQPM* (T, μ_q,p)

❑ n_B , χ_q at finite (T, μ_B)

$$\chi_q(T) = \left.\frac{\partial n_q}{\partial \mu_q}\right|_{\mu_q=0}; \quad \chi_q(T,\mu_q) = \frac{1}{9}\frac{\partial n_B}{\partial \mu_B}. \qquad \chi_2(T) = \frac{1}{9}\frac{1}{T^2}\left.\frac{\partial n_q(T,\mu_q)}{\partial \mu_q}\right|_{\mu_q=0} = \frac{1}{9}\frac{\chi_q(T)}{T^2}$$

for 3 flavours with $\mu_u = \mu_d = \mu_s = \mu_q$

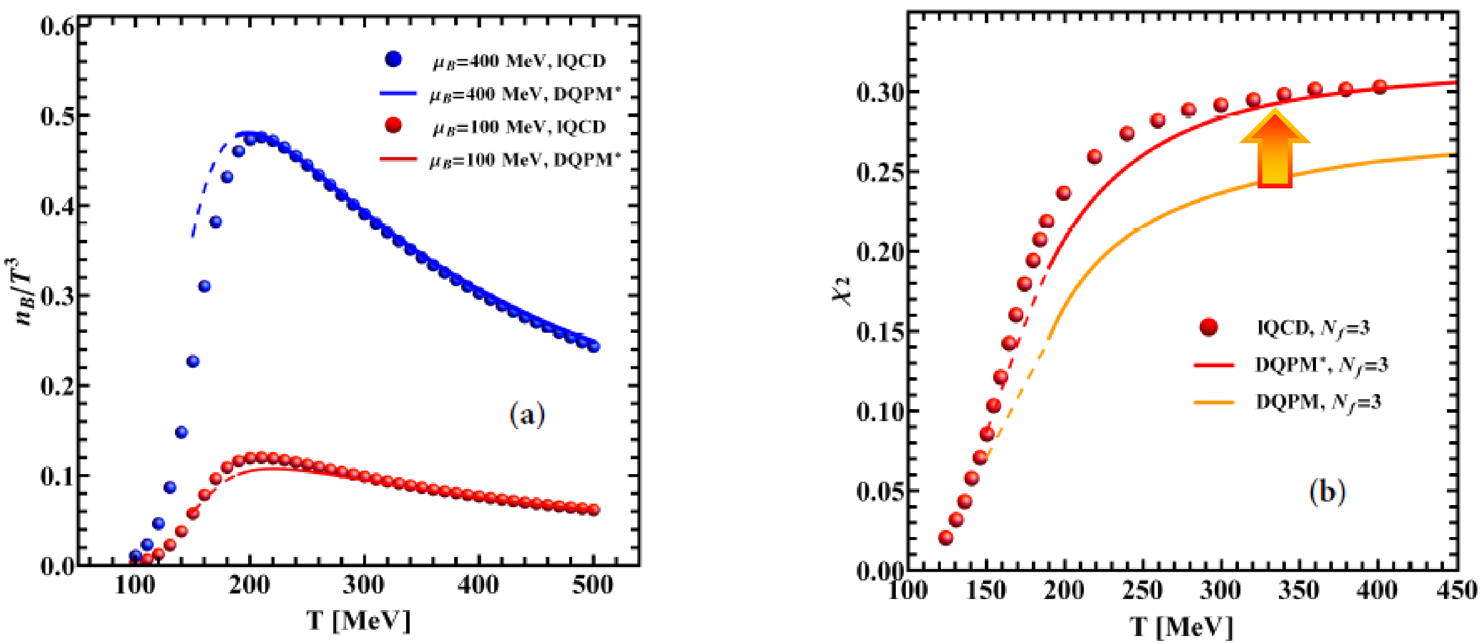

- **DQPM* describes n_B, quark susceptibility and entropy/pressure…**
- **p dependence of masses allows DQPM* to meet lQCD**

H. Berrehrah et al, PRC 93 (2016) 044914, arXiv:1512.06909; Int.J.Mod.Phys. E25 (2016) 1642003, arXiv:1605.02371

DQPM *(T, μ_q,p) :

transport properties at finite (T, μ_q)

(based on relaxation time approximation - RTA)

I. DQPM*: transport properties at finite (T, μ_q) : η/s

Shear viscosity η/s at finite T

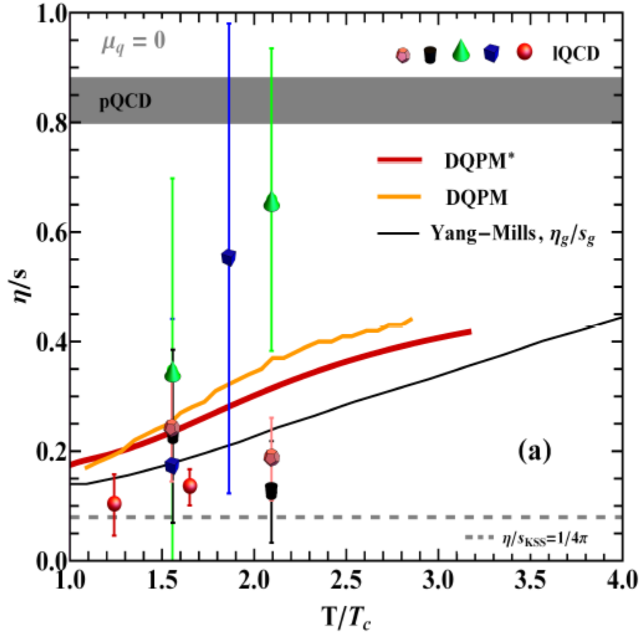

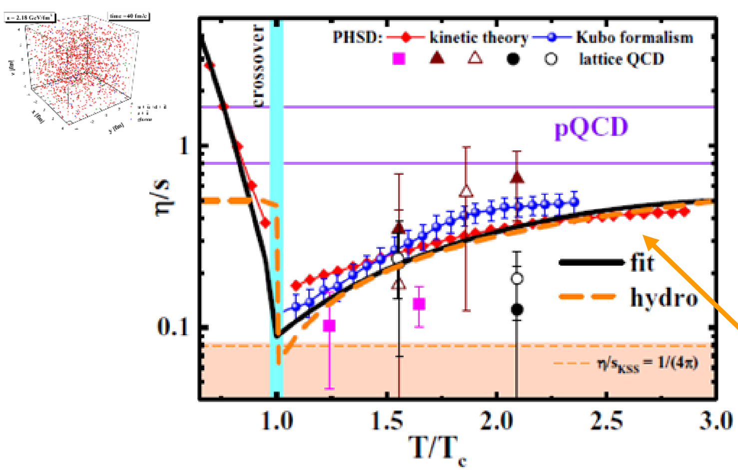

Shear viscosity η/s at finite (T, μ_q)

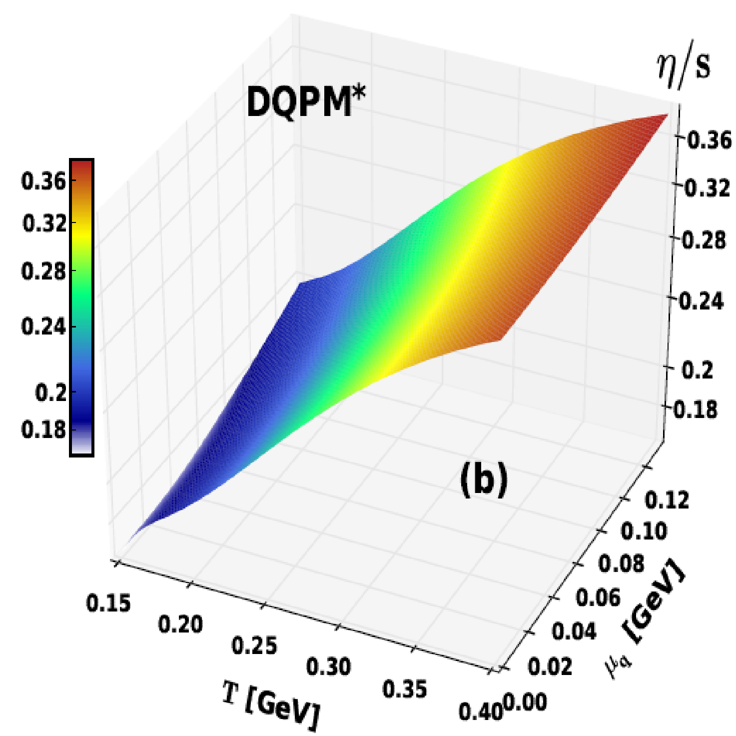

η/s: μ_q=0 ➔ finite μ_q:
smooth increase as a function of (T, μ_q)

H. Berrehrah et al, PRC 93 (2016) 044914, arXiv:1512.06909;
Int.J.Mod.Phys. E25 (2016) 1642003, arXiv:1605.02371

PHSD in a box: V. Ozvenchuk et al., PRC 87 (2013) 064903

II. DQPM*: transport properties at finite (T, μ_q): ζ/s

Bulk viscosity ζ/s at finite T

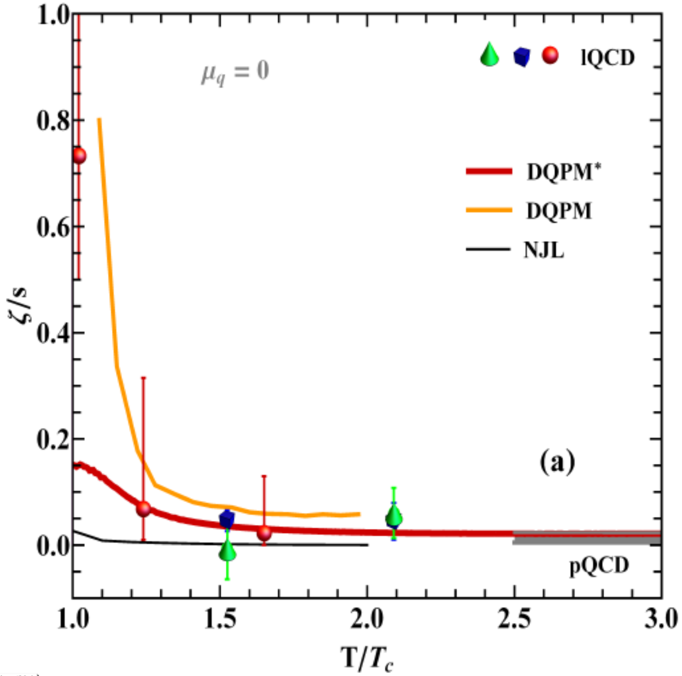

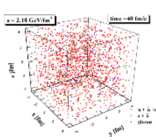

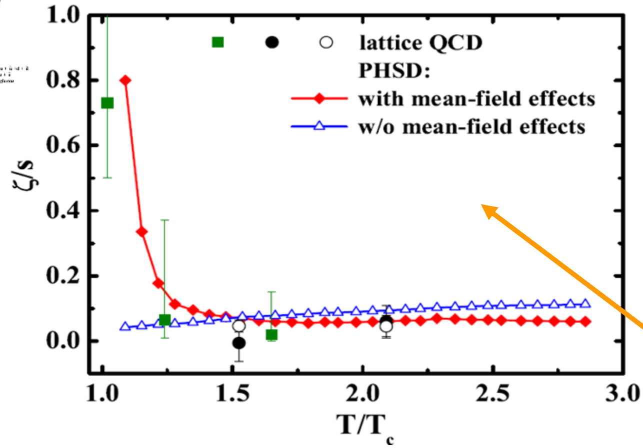

Bulk viscosity ζ/s at finite (T, μ_q)

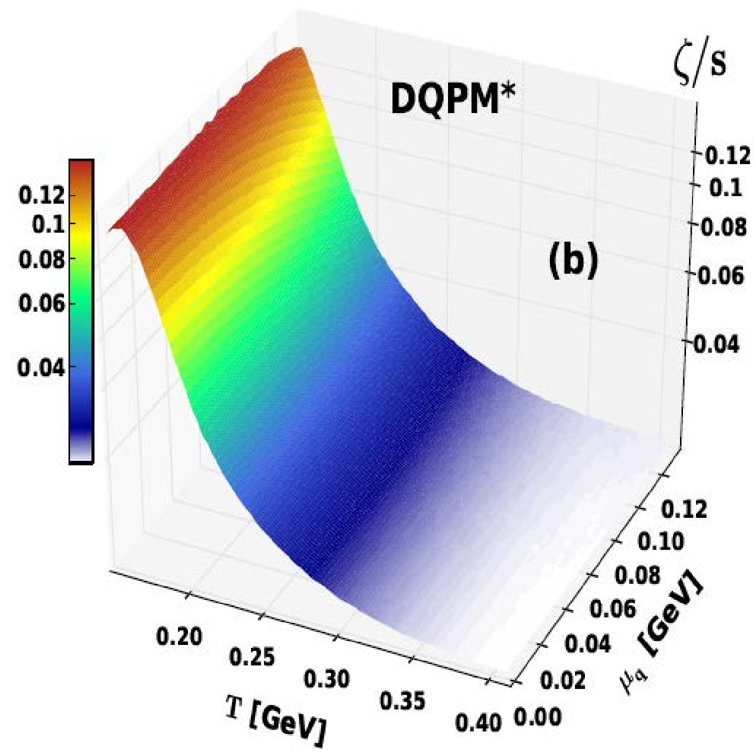

ζ/s : μ_q=0 ➔ finite μ_q:

smooth variation as a function of (T, μ_q)

H. Berrehrah et al, PRC 93 (2016) 044914, arXiv:1512.06909; Int.J.Mod.Phys. E25 (2016) 1642003, arXiv:1605.02371

PHSD in a box: V. Ozvenchuk et al., PRC 87 (2013) 064903

III. DQPM*: transport properties at finite (T, μ_q): σ_e/T

Electric conductivity σ_e/T at finite T

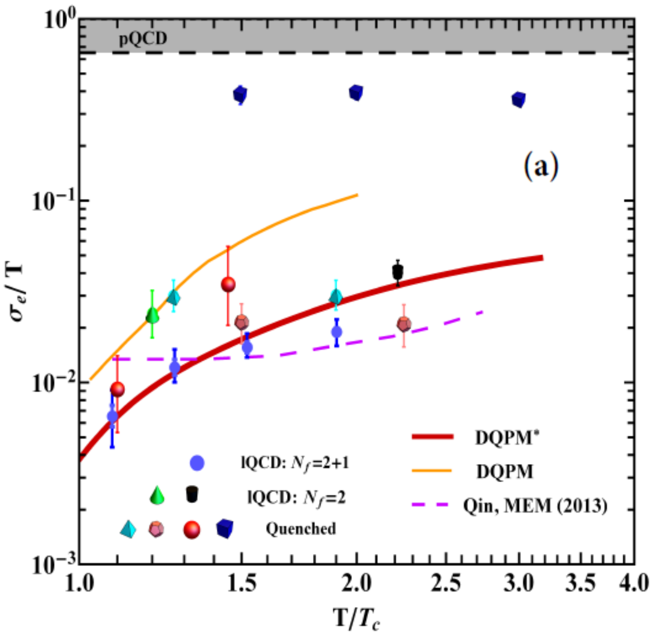

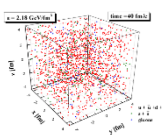

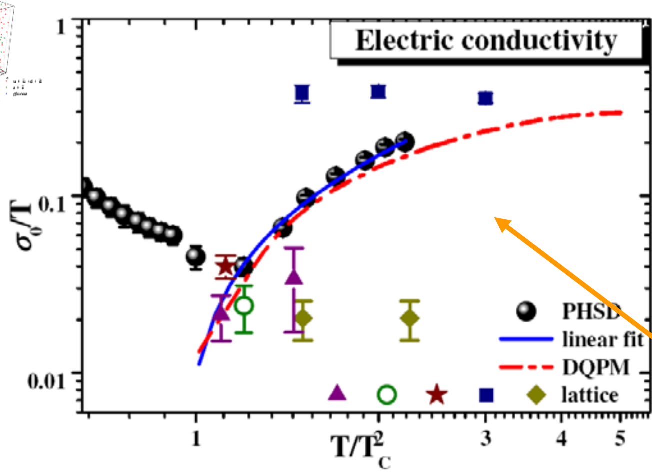

Electric conductivity σ_e/T at finite (T, μ_q)

$$\sigma_e(T,\mu_q) = \sum_{f,\bar{f}}^{u,d,s} \frac{e_f^2\ n_f^{\rm off}(T,\mu_q)}{\bar{\omega}_f(T,\mu_q)\ \bar{\gamma}_f(T,\mu_q)}$$

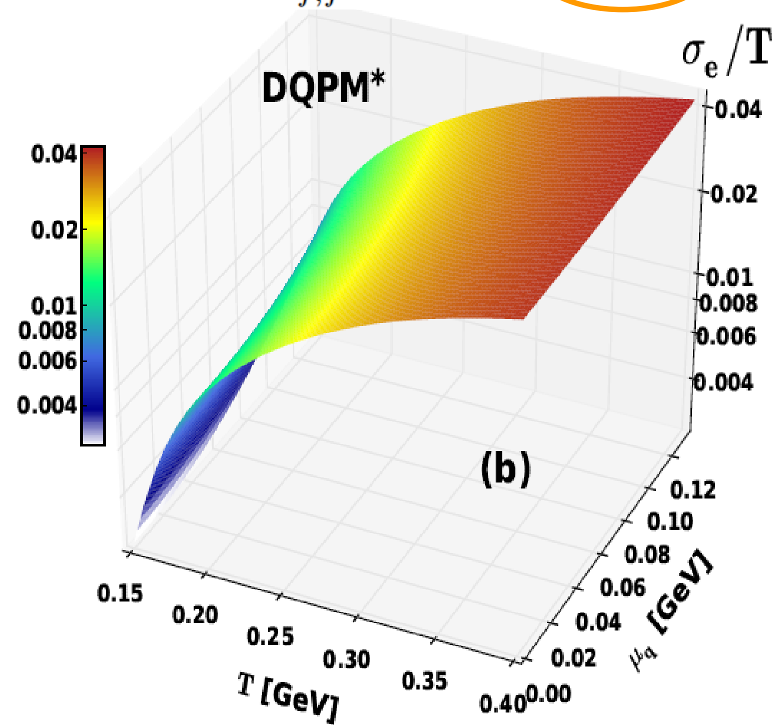

σ_e/T : μ_q=0 ➔ finite μ_q:
smooth variation as a function of (T, μ_q)

H. Berrehrah et al, PRC 93 (2016) 044914, arXiv:1512.06909; Int.J.Mod.Phys. E25 (2016) 1642003, arXiv:1605.02371

PHSD in a box: V. Ozvenchuk et al., PRC 87 (2013) 064903

Charm spatial diffusion coefficient D_s in the hot medium

- D_s for heavy quarks as a function of T for $\mu_q=0$ and finite μ_q

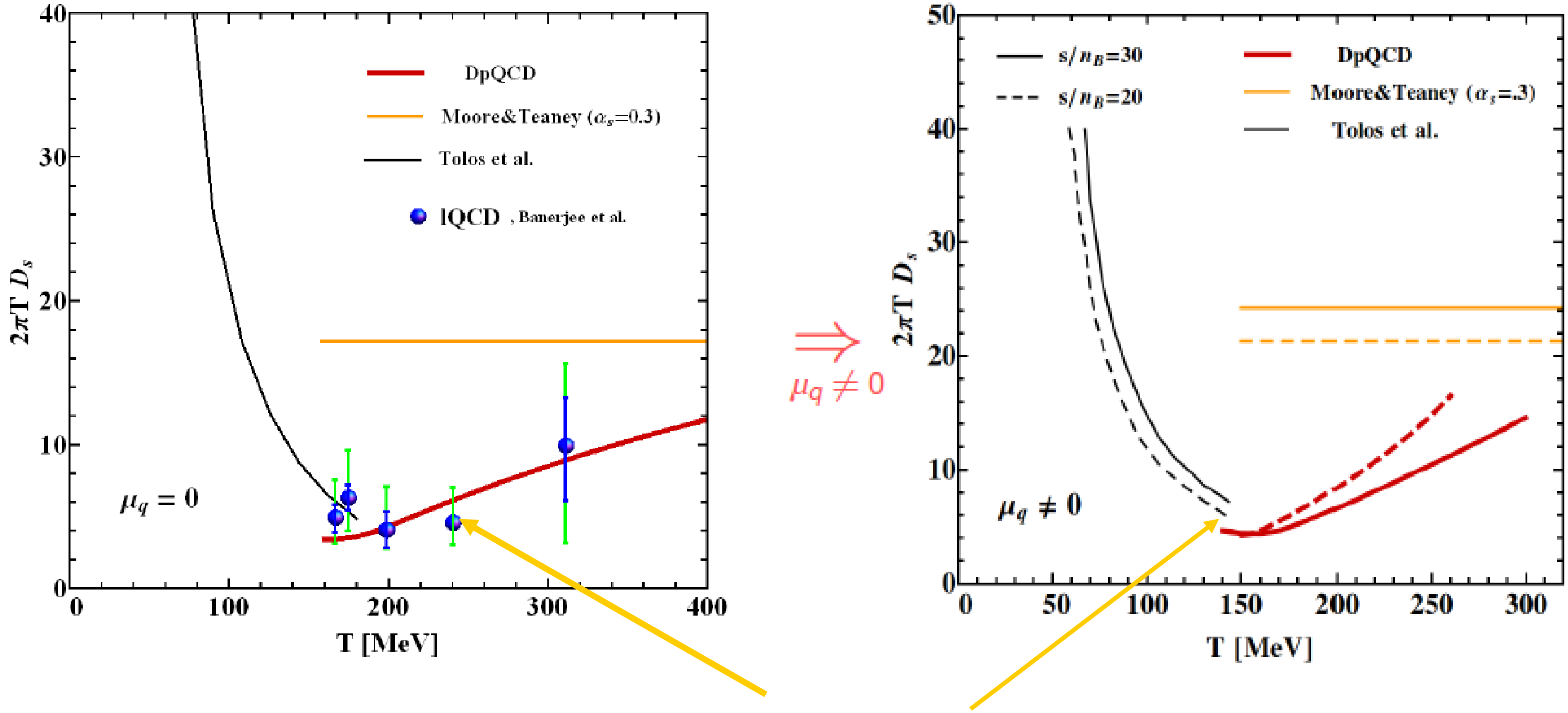

❑ T < T_c : hadronic D_s

L. Tolos , J. M. Torres-Rincon, Phys. Rev. D 88, 074019 (2013)

➔ Continuous transition at T_C!

H. Berrehrah et al, PRC 90 (2014) 051901, arXiv:1406.5322

Summary: DQPM, DQPM* at finite (T, μ_q)

- Extension of the **DQPM to finite μ_q** using **scaling hypothesis** for the effective temperature T*

- **μ_q=0 ➔ finite μ_q:**
  - variations in the QGP transport coefficients
  - **smooth dependence** on (T, μ_q)
  - η/s, ζ/s, σ_e/T, D_s show **minima** around T_C at μ_q=0 and finite μ_q

- **additional p dependence of masses allows DQPM* to meet lQCD:** DQPM* describes n_B, quark **susceptibility** and entropy/pressure…

- **Outlook**

Implementation into PHSD: from T,μ_q=0 ➔ finite T,μ_q

Thank you!


CPOD 2017
Critical Point and Onset of Deconfinement
Charles B. Wang Center - Stony Brook University
August 7-11, 2017